Review

Not peer-reviewed version

The use of newly formed minerals to characterize geothermal reservoirs and their cap rock: examples from intracontinental extensional basins and volcanic islands in subduction context

Béatrice A. Ledésert *

Posted Date: 31 August 2023

doi: 10.20944/preprints202308.2185.v1

Keywords: geothermal reservoirs; cap-rocks; exploration; clay minerals; quartz; carbonates; fluid inclusions; chlorite geothermometers; flow pathways

Review

The Use of Newly Formed Minerals to Characterize Geothermal Reservoirs and Their Cap Rock: Examples from Intracontinental Extensional Basins and Volcanic Islands in Subduction Context

Béatrice A. Ledésert

CY Cergy Paris Université, Geosciences and Environment Cergy, 1 rue Descartes, F-95000 Neuville-sur-Oise; beatrice.ledesert@cyu.fr

Abstract: Geothermal energy aims at harnessing the heat of the Earth to produce energy, from the near-surface to great depths. Emphasis is put on geothermal reservoirs in crystalline rocks, hence volcanic islands and crystalline basements of sedimentary basins based on three examples worldwide. Hot brines circulate in those rocks and are responsible for their hydrothermal alteration because of fluid-rock interactions. This includes dissolution of preexisting minerals and crystallization of newly formed ones which provide many information of crucial importance for a better exploration of those reservoirs. For example, the crystallization of clay minerals results from the dissolution of preexisting minerals (feldspar and ferro-magnesian minerals in plutonic, volcanic or metamorphic rocks) or from the direct precipitation from geothermal brines, in specific conditions. Clay minerals are found in both the geothermal reservoirs and in the clay-cap found above them. Other newly formed minerals such as quartz, carbonates or sulfates have also recorded the conditions of temperature and salinity encountered by fossil reservoirs which can be evaluated thanks to the study of fluid inclusions trapped during their crystallization. This paper presents results from several geothermal deep sites and surface analogues to pinpoint the role played by newly-formed minerals in the characterization of geothermal reservoirs and their cap-rock.

Keywords: geothermal reservoirs; cap-rocks; exploration; clay minerals; quartz; carbonates; fluid inclusions; chlorite geothermometers; flow pathways

1. Introduction

Geological energy resource reservoirs, including fossil fuels and geothermal energy, need to be thoroughly characterized before exploitation. In the global context of energy transition, the use of the heat of the earth to provide energy is of crucial importance. Deep geothermal exploitation needs three components to be found together: heat, water and flow pathways. Flow pathways are rather obvious in rocks that present matrix permeability and porosity like limestones and sandstone sin sedimentary basins. However, in geothermal reservoirs located in basement and volcanic areas, for heat or electricity production, the recognition of fluid flow pathways is of first importance. In those cases, the flow pathways are manly discontinuities (e.g. joints between lava flows in volcanic areas, debris flow layers [1,2], fractures (e.g. in volcanic [3] and granitic environments ([4–10]), and damage zones around them. In all of those zones, the natural circulation of hydrothermal fluids generates fluid-rock interactions [11] that can produce an increase in porosity and permeability [12] and hence improve the ability of fluids to circulate within the rock and create a geothermal reservoir. Fluid-rock interactions that occur in that case are responsible for the dissolution of preexisting minerals [12] and the crystallization of newly-formed ones [2,13,14] that can help determining the physico-chemical conditions reached by the reservoir [15] and the zones that produce hot water. In addition, they help locate the caprock responsible for the cover of geothermal reservoir that prevents too much hot water from leaking to the surface [16–21]. Several kinds of newly-formed minerals have already proven to be good proxies. Quartz is able to trap the fluids responsible for the hydrothermal alteration into fluid inclusions which can be studied by microthermometry [14,22–25] or crush-leach [26,27].

Preprints (www.preprints.org) | NOT PEER-REVIEWED | Posted: 31 August 2023 doi:10.20944/preprints202308.2185.v1

Carbonates, which are generally not found in fresh granite or volcanic rocks like andesite, are also produced during hydrothermal alteration in those environments, mostly by dissolution of plagioclase [5,9,28]. They sometimes also contain fluid inclusions. Clay minerals are very sensitive to the conditions of fluid-rock interactions and hence might provide an idea of the temperature reached by the reservoir ([13,14,29]. For example, chlorite can be used as a geothermometer and several examples are found in the literature [30,31]. Their use, combined with fluid inclusions, for example in quartz, can help showing the cooling of a paleo-hydrothermal reservoir [14] and hence provide a model for the evolution of present-day geothermal reservoirs. In addition, the porosity that is created between the clay crystallites promotes matrix permeability [12,13,25] and is favorable to geothermal projects. Finally, carbonates and clay minerals can be dissolved by acid injection during the chemical stimulation of geothermal wells to enhance the permeability around them. Hence, these three types of minerals are actively searched for during geothermal exploration. This paper focuses on volcanic environments and crystalline basement of sedimentary basins based on three examples worldwide (Figure 1), namely Soultz-sous-Forêts (Upper Rhine Graben, URG) and its surface analogue (Noble Hills, California, USA), and Guadeloupe (Bouillante geothermal field and its Terre-de-Haut surface analogue) to show the use of some mineral species for a better exploration of geothermal reservoirs and the relevance to study surface analogous systems ([6,7,7,32,33] when few information is available from geothermal boreholes or when none is available. It will be composed of four main sections including the geological context of the two major geological environments (section 2): intra-continental extension basins with examples from the Upper Rhine Graben (URG, France) and the Basin and Range section in Death Valley (DV, California, USA), and volcanic setting in the Lesser Antilles (Guadeloupe, France). Then, three sections will be dedicated to mineral species: clay minerals (section 3), carbonates (section 4) and finally quartz (section 5).

Figure 1. Location map of the three sites on which this review is based, in two different geological contexts: intra-continental extension basins (Upper Rhine Graben, URG, and Death Valley, DV) and volcanic islands (Basse Terre of Guadeloupe and Terre-de-Haut in Les Saintes, both in Lesser Antilles).

2. Geological settings of chosen sites

2.1. Extensional basins in continental domains: examples of the Upper Rhine Graben (France) and Death Valley (USA)

2.1.1. Upper Rhine Graben (URG)

The Upper Rhine graben is the central part of the European Cenozoic Rift System [34]. It is 300 km in length about 50km in width. It extends from Basel (Switzerland) to Mainz (Germany) in a NNE-SSW direction, and covers the eastern part of France (Figure 2). It hosts several thermal anomalies [34–36] associated with natural brine circulation through a nearly vertical fracture network which crosscuts Triassic sediments overlying the Paleozoic crystalline basement [37–39]. Fifteen deep wells were drilled in the URG over more than 30 years to harness thermal anomalies for geothermal

Preprints (www.preprints.org) | NOT PEER-REVIEWED | Posted: 31 August 2023 doi:10.20944/preprints202308.2185.v1

purpose [11,40–42]. The Palaeozoic granitic basement is made of several types of granite: mainly a porphyritic monzo-granite locally affected by intense vein alteration and a two-mica granite crosscut by Soultz-sous-Forêts (called Soultz in the following) and Basel deep drillholes [11] (Figure 2). The enhanced geothermal system (EGS) project at Soultz was initiated in the 1980s to develop a deep fractured granitic reservoir [43]. Crystalline rocks being generally characterized by low matrix porosity, the main flow occurs in permeable and connected fractures either in the basement or it sedimentary cover [44,45]. Thus, projects based on EGS technology require a good knowledge of the fracture network to understand flow distribution at depth and to design borehole trajectories according to the geometrical properties of the fracture network [46]. In the Soultz granite, the porosity of 25% measured in the bulk rock of an altered halo around a fracture [25] was associated with high permeability [12]. In this zone, the primary crystals of the granite were totally replaced by an assemblage of carbonates, clay minerals and newly-formed quartz. Hence, a specific mineralogical signature of paleo-fluid circulations is encountered. At Rittershoffen, 10 km away from Soultz, the high-temperature anomaly is concentrated around Rittershoffen fault, which probably hosts the main hydrothermal circulation [36,47]. The surface installations produce heat at Rittershoffen (24 MWth) and electricity at Soultz (1.5 Mwe). Other geothermal plants are located in Germany in Insheim (4.8MWe), Landau (2.9 MWe and 3 MWth), Bruchsal (0,5 MWe), and Brühl (Figure 2).

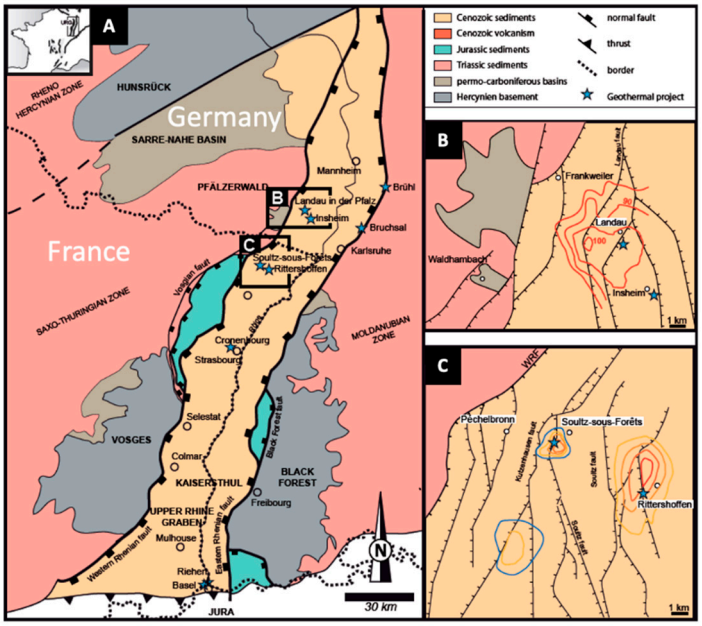

Figure 2. – Geological setting of extensional basins in continental domains : the Upper Rhine Graben (A) with a focus on thermal anomalies on the German side (B) and the French side (C). Modified after [48].

2.1.2. Death Valley with a focus on the Noble Hills

The Death Valley (DV; Figure 3) is also located in a Cenozoic system, about 700 km long with dextral strike-slip and extension [49–53]. This northwest-trending system is located between the Basin and Range region to the east and the Sierra Nevada batholith to the west [51]. Today, it accommodates ~25% of the Pacific-North America relative motion [49,53,54]. It has been formed by a right-lateral movement giving a pull-apart structure [55]. The Noble Hills (NH), located in the southern part of the DV region, trend parallel to the Southern DV Fault Zone (SDVFZ). Geological markers along the SDVFZ trace [56] suggest that the NH correspond to a transported fragment of the frontal part of the Owlshead Mountains (OM), a Cretaceous (~95 Ma, [57]) granitic pluton at a 40–41 km distance to the SE. The NH are composed of Proterozoic sediments (quartzite, dolomite, detrital flysh, and carbonate sequences) crosscut by 1.1 Ga diabase sills, the whole being intruded by Mesozoic granite [58] in which important signs of hydrothermal alteration were discovered [6] along fracture patterns

Preprints (www.preprints.org) | NOT PEER-REVIEWED | Posted: 31 August 2023 doi:10.20944/preprints202308.2185.v1

characterized by [7,59]. In [6,7,32,59], the Noble Hills granite is considered as a surface analogous system to the Soultz site and allows a 3D study of fracture systems and their related hydrothermal alteration which is hardly possible in Soultz wells.

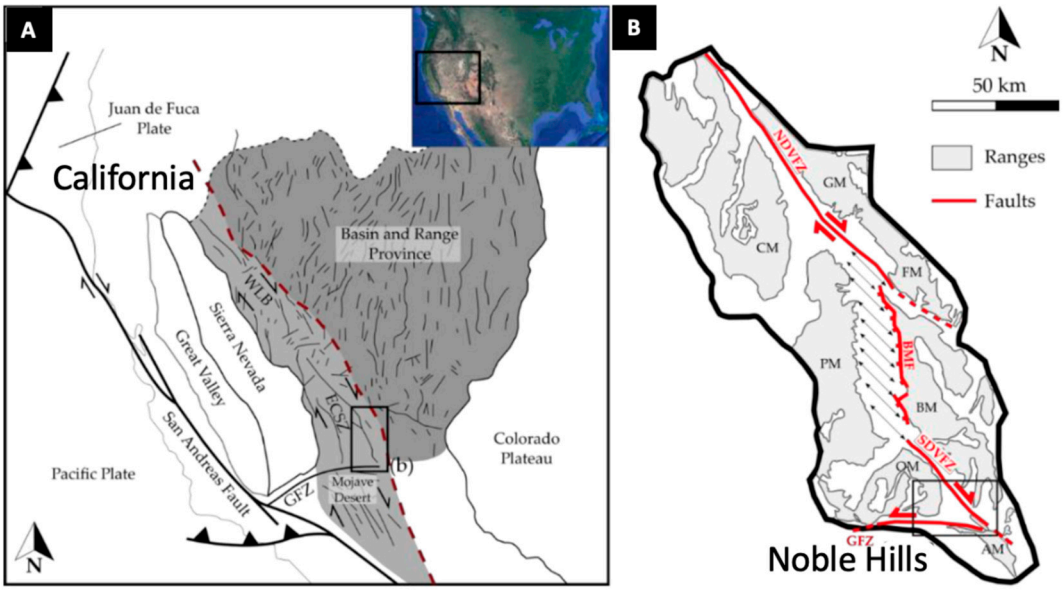

Figure 3. – Location and geological map of Great Basin region (western U.S. Cordillera) showing (A) WLB—Walker Lane Belt; ECSZ—Eastern California Shear Zone; GFZ—Garlock Fault Zone. The Basin and Range Province is represented in dark grey and the Death Valley (WLB/ECSZ domain) in light grey, between the Basin and Range region to the east and the Sierra Nevada batholith to the west. The red dashed line marks the limit between these two domains. The dark lines within the Basin and Range Province and in the WLB-ECSZ zone represent the main faults. (B) Structural setting of the Death Valley region (modified after [33,34]) showing from north to south the various mountain massifs: GM—Grapevine Mountains; CM—Cottonwood Mountains; FM—Funeral Mountains; PM—Panamint Mountains; BM—Black Mountains; OM—Owlshead Mountains; AM—Avawatz Mountains; and for the faults, from south to north: GFZ—Garlock Fault Zone; SDVFZ—Southern Death Valley Fault Zone; BMF—Black Mountains Fault; NDVFZ—Northern Death Valley Fault Zone. The Noble Hills which are reported here are located in the horizontal black rectangle, south of the map (B). Modified after [6].

2.2. Volcanic islands: two examples in Guadeloupe archipelago (Bouillante geothermal power plant and its surface analogue in Terre de Haut, Les Saintes).

Guadeloupe archipelago

1. Bouillante

The Bouillante geothermal power plant (Figure 3) is located on the west coast of Basse-Terre island, in the inner active part of the Lesser Antilles arc [60] that results from the subduction of the North American plate under the Caribbean plate at a velocity of approximately 2 cm.yr^{-1} [61–63]. The Bouillante geothermal field was brought into production in 1986 and increased its production capacity up to 15 Mwe in 2005, representing about 7 % of the island's annual electricity needs [64]. In 2019, the production of electricity was nearly 110.000 MWh [65]. The Bouillante field is located at the western end of a volcano-tectonic depression belonging to the Marie-Galante graben system limited by the N090-N120 Bouillante-Capesterre regional fault that is found immediately north of Bouillante [66]. This extensive structure is bounded offshore to the west by a major N140-170 fault linking the normal-sinistral Montserrat-Bouillante system to the north with the Les Saintes system to the south [67]. The Bouillante field is contained within an andesitic volcanic substratum. Its high-enthalpy hydrothermal system is emplaced in submarine volcanoclastic formations (mostly hyaloclastites) and subaerial formations (andesitic lava flows, pyroclastites, lahars). It has undergone

Preprints (www.preprints.org) | NOT PEER-REVIEWED | Posted: 31 August 2023 doi:10.20944/preprints202308.2185.v1

hydrothermal activities of several types from high temperature, up to 245°C [66] to low temperature episodes (<100°C, [68]). The Bouillante field is related to the volcanic activity of the Axial Chain complex (1.023 to 0.445 Ma volcanic deposits; [69]) the Bouillante Volcanic Chain (*c.* 0.850–0.250 Ma ago after adularia dating; [70]) and the presently active Grande Découverte–Soufrière system (0.200 Ma ago–present day;). The Bouillante hydrothermal event is related to changes in the magmatic history of the studied area, with at least two volcanic pulses [70].

2. Les Saintes, Terre-de-Haut island

Terre-de-Haut island belongs to Les Saintes sub-archipelago located south-east of Basse-Terre of Guadeloupe. It is considered as an exhumed fossil analog system to the buried Bouillante's geothermal field. Verati et al. (2016) [3] recognized four families of fault systems, active from 3 to 2 Ma, displaying normal-slip movements, and three of them (excluding the N090-N110 direction) also show a strike-slip movement. These four families of fault systems are consistent with the global tectonic framework of the entire Guadeloupe archipelago (see above about Bouillante and in [3]).

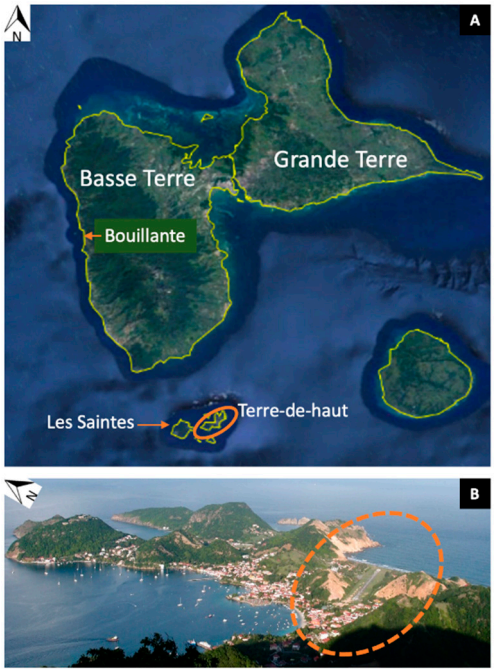

Figure 3. – Location map of Bouillante geothermal site in Guadeloupe and of Terre-de-Haut island (orange ellipse) in the Les Saintes sub-archipelago used as its surface analog (A). Focus on the hydrothermally-altered area in Terre-de-Haut surrounded by a dashed orange ellipse (B) : in this zone the altered rocks are yellowish instead of brown like in the northern part of the island where the rocks are much fresher.

New structural, petrographic and petrophysical data were published recently [1,3,13,71]. Geochronological data [71] revealed the presence of three main subaerial volcanic phases on Terre-de-Haut, from 2.98 ± 0.04 Ma to 2.00 ± 0.03 Ma. The occurrence of a hydrothermally-altered zone was recently accurately documented in terms of nature of hydrothermalism, duration of the event and cooling of the system [3,13,14,29]. According to [3], the intersection of the two major normal fault systems (N090-N110 and N130-N140) is responsible for the development of this hydrothermally-altered area, which is also the case in the Bouillante geothermal field [66]. This hydrothermally-altered zone displays a succession of parageneses that are characteristic of high-temperature hydrothermal alteration in epithermal settings and its retrogression during cooling [3,13,14,29]. In their study of clay mineral assemblages in the hydrothermal zone of Terre-de-Haut, [13] showed a horizontal zonation with illite and chlorite isograds. This clay mineral distribution is commonly observed in geothermal contexts and is similar to that observed vertically in Bouillante's boreholes [66].

3. Clay minerals

Clay minerals are among the most ubiquitous minerals found in the volcanic and crystalline basement environments discussed in this paper, in which they are issued from hydrothermal or surface alteration processes. Their study is spread worldwide and for multiple applications, among which the location of clay-cap or cap-rock of geothermal systems, the characterization and better knowledge of geothermal reservoirs and their evolution through time

3.1. Cap rock: Electrical resistivity, gravimetry and magnetotelluric exploration

The underground circulation of hot water, of interest for geothermal energy production, is often indirectly inferred from the presence of minerals formed by hydrothermal alteration at different temperatures. Clay minerals, such as smectite and chlorite, can be mapped from the surface using electrical soundings and give information about the structure of the geothermal system, for example on Krafla volcano (Iceland) [19,20]. Their massive occurrence close to the surface shows the presence of a clay cap that forms an impermeable lid over the geothermal reservoir as visible in [66] and reported by [68]. Strangway et al. (1973) [72] were among the first ones to use audio-frequency magnetotellurics to reveal low-resistivity bodies. It is now widely processed for geothermal exploration (e.g. [73–76]. Levy et al. (2018, 2019) [19,20] compared frequency-domain electrical properties in borehole and in laboratory on samples to investigate the specific role of smectite in the electrical response of igneous basaltic rocks. They evaluated what physical processes make smectite a better electrical conductor than surrounding minerals in the active hydrothermal system at the Krafla volcano, in Iceland. They showed that cation exchange capacity (CEC) is found to be a reliable measure of the smectite weight fraction in these volcanic samples. They compared this value with an independent quantification of the smectite content using X-ray diffraction. In Guadeloupe at Bouillante, [77] interpreted the resistivity distribution from electromagnetic surveys in terms of water saturation of rocks, hydrothermal alteration and presence of hydrated minerals, hence in that volcanic context likely resulting from hydrothermal alteration. They also used gravity to distinguish and characterize the denser formations from the low-density areas. Combining both these approaches, they showed a layering of the geological formations in the geothermal system. The shallow resistive layer they observed is explained in terms of recent massive volcanic formations, while the conductive intermediate layer marks the low density, demagnetized clay cap of the altered geothermal system.

In Italy, [17] performed mineralogical investigations on the cap rock of the geothermal system located close to Vico volcano to assess its effectiveness and degree of interaction with fluids. In this system, a low permeability siliciclastic cap rock overlies a permeable carbonate reservoir. Where it is unfractured, the cap rock shows maximum paleo-temperatures interpreted as the thermal signature of the original cold sedimentary basin. Where it is fractured, it is characterized by an assemblage of kaolinite, calcite, mixed layers illite-smectite. The temperature assessed in those fractures is between 85 and 140°C indicating a strong interaction with hot fluids from the carbonate reservoir. Clay recrystallization occurred along the walls of tensile fractures pre-dating the active hydrothermal system which acted as passive anisotropies that focused localized alteration. The compositional and structural changes in mixed layers I-S are shown to be function of hydrothermal fluid temperature.

3.2. Geothermal reservoirs

Clay minerals are renown for resulting from hydrolysis of preexisting minerals in various geological environments, hence whatever the nature of rocks and the temperature of the environment in which they formed, from the soil [78] to high-enthalpy geothermal systems [68,79]. Recently [80] showed how the clay mineralogy can be used as a signature of granitic geothermal reservoirs of the central Upper Rhine Graben (URG) at Soultz and Rittershoffen. Before that, [9,25,81] showed the abundance and variety of clay minerals in hydrothermally transformed zones of the Soultz granite while [82] indicated the significance of hydrothermal alteration zones for the mechanical behavior of a geothermal reservoir.

 doi:10.20944/preprints202308.2185.v1

3.2.1. Types of hydrothermal alteration

1. Propylitic alteration

In the Noble Hills, away from the fractures, the granite underwent pervasive propylitic alteration [32]. This type of alteration is described as isochemical by [83] and hence occurs in rock-dominated systems. It is characterized by a calcite-corrensite-epidote-K-white mica assemblage in the Noble Hills [32] while amphibole and biotite are partly transformed into chlorite + carbonate ± epidote or hydrogrossular and plagioclase into calcite + corrensite or illite at Soultz [25]. At Bouillante, it affects all parts of the system and consists of crystallization of trioctahedral phyllosilicates (chlorite or corrensite), Ca-silicates (heulandite-clinoptilolite, prehnite, pumpelleyite, wairakite and epidote), quartz and minor calcite in replacement of most of the primary minerals of the intersected volcanic or volcanoclastic formations [79]. These assemblages are classical in propylitic alteration. Indeed, [83] indicate a limited number of phases : K and Na-feldspars, muscovite, quartz, c1ays (including chlorite), epidote, prehnite or calcite, the proportion of which depended upon the initial chemical composition of the rock, but is independent of the initial fluid composition. Berger and Velde (1992) [83] determined the chemical parameters controlling the propylitic and argillic alteration process using the EQ3/6 software package.

2. Argillic alteration

BergerVelde (1992) [83] obtained the extreme argillic facies parageneses (quartz, kaolinite) by modeling using the EQ3/6 software package at temperatures < 200°C, water/rock ratios > 10^3-10^2, and with acid solutions, by reacting the propylitic mineral assemblages and their coexisting fluids with imposed chemical variables (fCO_2, fS_2, salinity). In the field, the argillic facies is found worldwide.

At Soultz, the granite underwent intense hydrothermal alteration, as pinpointed by the local total dissolution of plagioclase (oligoclase), biotite, amphibole and quartz and the crystallization of a mineral assemblages made of illite, calcite and other carbonates, quartz, and tosudite (see 3.2.2 and [25]). This vein argillic alteration was compared with the reference facies (propylitized granite) in order to show gains and losses of elements during alteration, hence deducing that it occurred in an open system. The geochemistry of the brine circulating at present [84,85] is characterized by a high salinity (ca 100g/L) due to a great abundance of Na, K and Ca as major cations and Cl and SO_4 as major anions. Li, Zn, Ba and other minor elements are also present in significant abundance (173 mg/L, 2168 µg/L and 5070 µg/L respectively, [86]). In addition, the geothermal fluid is characterized by a high CO_2 content, and natural anoxic conditions [85,87]. Geochemical modelling of the fluid–rock interactions based on thermodynamics and kinetics of reactions with this present-day fluid collected in the Soultz geothermal reservoir with a temperature of 140°C showed that this brine is indeed able to precipitate illite from the alteration of plagioclase [88].

In the Noble Hills granite, close to the fractures within which hydrothermal fluids circulated, illite, kaolinite, illite/smectite, calcite and oxides, characteristic of the argillic alteration, were encountered, which overprinted the propylitic alteration [6]. Alteration was also outlined by the correlation of the loss on ignition, representing the hydration rate, to porosity, calcite content and chemical composition such as Na depletion due to plagioclase alteration and a K enrichment associated to illite precipitation. Moreover, the Noble Hills granite shows signs of several generations of fluid circulations resulting in successive veins of various mineralization (quartz, carbonates, barite). The porosity, the calcite content, and the temperature indicated by the Kübler Index calculated from the crystallinity of illite increase together near fracture zones.

The Bouillante geothermal wells go down to a depth of 1000 m where temperatures exceed 250 °C [79]. These authors paid special attention to the clay content of fractured zones which channel the present-day geothermal fluids. They identified three successive zones, dominated, respectively by dioctahedral smectite, illite and chlorite at increasing depths resulting from the spatial superimposition of at least two successive alteration stages. The first one is of propylitic type (see section 3.2.1.1). The later stage of alteration is related to the circulation of the present geothermal fluids and is assimilated to argillic or phyllic alteration. It consists of a more or less intense argillization which results from the crystallization of aluminous dioctahedral clay phases (smectite, illite±I–S mixed layers, and accessory kaolinite) associated with quartz, calcite, hematite or pyrite.

Preprints (www.preprints.org) | NOT PEER-REVIEWED | Posted: 31 August 2023 doi:10.20944/preprints202308.2185.v1

The permeable zones which channel most of the present geothermal fluids are fracture controlled and do not contain specific clay parageneses. However, the illite ± I–S mixed layers minerals differ from those of the surroundings by specific properties including both crystal structure and texture. These specific properties (decrease in the expandable component of the illitic material, increase of the illite crystallinity) can be controlled by the nucleation/growth rates operating in zones of active flow regime. Being mainly a product of the earlier propylitic alteration stage, chlorites are much less informative on the fracture controlled permeable levels. However, the compositional variations of chlorites recorded within the shallower fractured zone suggest a significant change in fO2 conditions related to early circulation of fluids along the major near west striking normal faults (Plateau fault).

In all of these cases, a clear link has been established between the argillic alteration and the fracture system which has generally been thoroughly studied like at Soultz [9,10,25,89], in the Noble Hills [6,7,59] and in Guadeloupe [1–3,13]. As an example, a compiled map is provided here (Figure 4) on which the mineralogy after [13] was superimposed over the location of the hydrothermally-altered zone and structural data of [3]. It shows a clear relationship between the fracture network and the distribution of clay minerals. The chloritic hot core is located at the intersection between two fractures oriented N100 and N140. The southernmost isograd of illite appearance (Ilt+) is clearly modeled on fractures and normal faults.

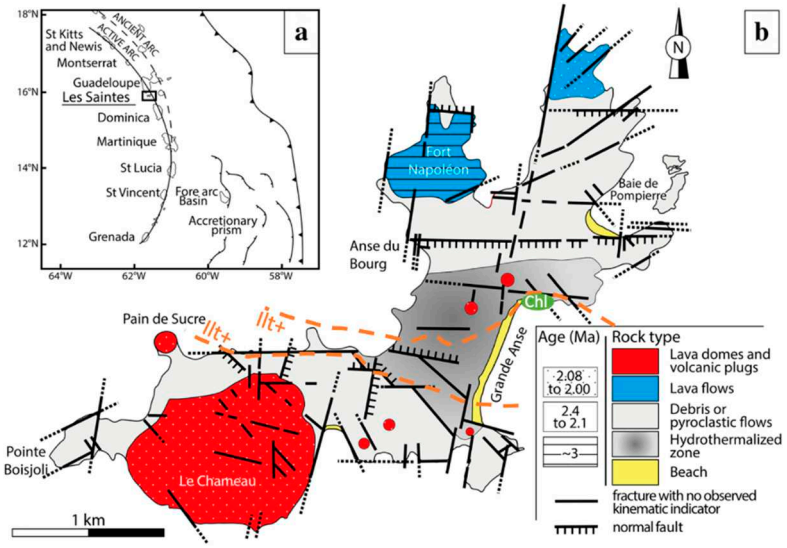

Figure 4. – Compiled map showing the clear relationship between the faults and fractures, petrography in terms of hydrothermally-altered zone [3] and clay mineralogy [13]. The only zone where chlorite (Chl, green ellipse) is found on the island can be considered as the hotter zone and hence the core of the hydrothermal area when compared with Bouillante [66]. It is located at the intersection between two fractures oriented N100 and N140. In addition, the southernmost isograde of illite appearance (Ilt+, orange dashed line) is clearly modeled on fractures and normal faults. Illite is found between the two orange dashed lines (isograds labeled Ilt+). Outside those isograds, the clay mineral assemblages are dominated by smectite [13].

3.2.2. Tosudite, a specific lithium-rich clay mineral

In the Soultz granite harnessed for geothermal energy, tosudite was found in highly altered zones of the granite, close to faults in which quartz veins formed [25,90]. Tosudite, a di-dichlorite-di-dismectite mixed layer clay mineral [90] indicates the presence of lithium in the brine from which it crystallizes (see § 3.2.2.1 - 1). It is a rather rare mineral even though several occurrences have already been encountered worldwide in various environments like granites [90–92], rhyolitic rocks [93], altered wall-rocks of gold-bearing veins developed in tuffs [94], or very low-grade metamorphic grauwackes [95]. At Soultz, chemical analyses of tosudite pseudomorphous after plagioclase show 1.02 Wt% Li_2O [25,81]. In Li-rich environments, it is found instead of kaolinite in argillic alteration [25] and hence is a good indicator of the chemical content of fossil brines when geothermal reservoirs

Preprints (www.preprints.org) | NOT PEER-REVIEWED | Posted: 31 August 2023 doi:10.20944/preprints202308.2185.v1

are no more active. Where they are still active, Li which is a high-value element for electric batteries can be extracted together with geothermal energy [96,97]. In addition, tosudite is responsible for the local important porosity of the rock matrix as shown in Figure 5, and hence permeability [12], together with illite (Figure 5) as also showed for other geological environments like in Terre-de-Haut [13].

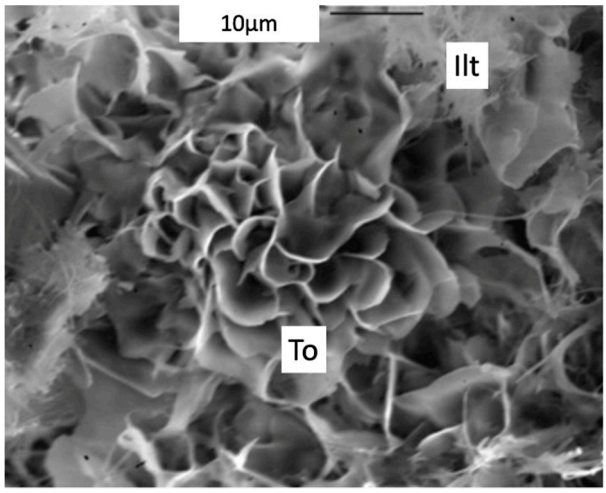

Figure 5. – Scanning electron micrograph showing the alveolar structure of tosudite (To) and hairy illite (Ilt), and hence the high bulk rock porosity (up to 25% [25]) of the altered wall rocks of fractures encountered in the Soultz granite. This porosity is correlated with high permeability [12].

3.2.3. Chlorite geothermometry

Chlorite crystals can be used for geothermometry in order to determine the temperature reached by geothermal reservoirs, provided they are found in association with quartz. Beauchamps et al. (2021) [14] applied this method to Terre-de-Haut to estimate the crystallization temperature of chlorite using the geothermometer developed by [30] specifically for low-T and low-pressure contexts (T < 350 °C and pressures below 4 kbar). This semi-empirical thermometer is based on a ratio of end-member activities and directly linking the temperature to a K constant for a chlorite + quartz equilibrium. This choice was driven by the low P-T conditions prevailing in the studied area, and the Si-rich composition of the Terre-de-Haut chlorites, preventing from the use of thermodynamic models such as that developed by [98]. In addition, the geothermometer developed by [30] does not require a prior quantification of the Fe^{3+} content, assuming that all iron is divalent. The thermometer developed by [31] can also be used provided the Fe^{3+} proportion is quantified for each chlorite analysis, which might be difficult to obtain. In Terre-de-Haut, the thermometer developed by [31] was used by [99] to determine cooling conditions of the paleo-geothermal reservoir and it was coupled with microthermometry of fluid inclusions in a euhedral quartz crystal indicating as a whole (i) a temperature of at least 240–270 °C in fluid inclusions trapped in the core of the quartz crystal, (ii) chlorite formation at about 120 °C, and (iii) temperatures of ca 50 °C in fluid inclusions of the quartz outer growth zones.

3.2.4. Use of illite (and muscovite).

1. Determination of temperature conditions using the Kübler Index

The Kübler index allows to determine the temperature conditions reached by geological systems, in particular sedimentary, and hence if they reached diagenesis only or metamorphic conditions. Its calculation is based on the mean thickness of the coherent scattering domain of illite crystals from X-ray diffraction full width data at half maximum (FWHM) intensity [100].

For example, in the Noble Hills, the Kübler Index was calculated from illite crystallinity and allowed to identify a NW-SE temperature gradient in the Noble Hills, related to propylitic alteration and to the thermal and tectonic history of this zone [32].

2. Dating of hydrothermal or metamorphic events

Among clay minerals, illite contains large amounts of potassium (K) which can be used for dating thanks to K/Ar ou Ar/Ar method. Even though it is not a clay mineral species, muscovite is another type of phyllosilicate which contains K and can also be dated.

For examples in the geological contexts considered here, [101] dated illite for the reconstruction of the thermal history of the Lower Triassic sedimentary rocks that crop out in the western shoulder of the URG or are deeply buried and overlain the granite basement in the URG. Two episodes of crystallization could be identified at Soultz at ~95 and 70 Ma, hence before the Miocene rifting. Dating performed on illite fractions extracted from the granite in the highly altered zone where tosudite was first described at Soultz indicates that illite crystallized during two episodes at 63 and 18 Ma [90], hence before rifting for the first episode and during it for the second one. The geochemical simulations performed by [88] indicate that the brine circulating at present in the fracture network of the Soultz granite is able to promote the crystallization of illite from the alteration of plagioclase. Hence illite precipitation might continue at present.

Favier et al. (2021) [102] performed Ar/Ar dating of hydrothermal muscovite developed in Terre-de-Haut island during pseudomorphic transformation of pyroxenes within altered rhyodacites at temperatures above 300 °C, hence probably corresponding to the high temperature event also described thanks to fluid inclusions in quartz (see section 5). The white micas display an age of ca 2.59 Ma corresponding to a high temperature fluid circulation in Terre-de-Haut geothermal paleo-reservoir. The whole temporal dataset reported by [102] implies a fast-cooling rate (>150°C/200 ka) and a maximal lifetime of 650 ka for Terre-de-Haut hydrothermal system.

3.2.5. Deciphering meteoric and hydrothermal alteration based on clay minerals

Surficial clay minerals as indicators of present-day geothermal activity were studied around Bouillante by [78] on >100 samples collected over and around the Bouillante geothermal system. Among the three types of mineral associations, that composed of kaolinite-smectite mixed-layered clays ± halloysite ± kaolinite ± smectite ± silica was found both within and beyond the bounds of the known geothermal area, suggesting a pedogenic origin. Hence, it is interpreted as a background of clayey tropical weathering (kaolinite-smectite) with a hydrothermal overprint characterized by dioctahedral smectites (beidellite) and illite-smectite. In addition, in the wells drilled in the Bouillante geothermal field [103] used scanning electron microscopy, electron microprobe analysis, X-ray diffraction (XRD), Fourier transform infrared spectrometry (FTIR), and oxygen-isotope analysis to study the montmorillonite-beidellite transition. They showed that beidellite precipitated from the hot geothermal fluid while montmorillonite precipitated from reacting solutions originating from the phreatic water table (± seawater) with minor contribution from the boiling zones. It appears that the montmorillonite vs. beidellite ratio of the smectite material is rather due to the mixing rate of geothermal fluid with meteoric waters than to depth.

In the Death Valley, weathering was evidenced in the Owlshead Mountains only (and not in the NH) by the presence of montmorillonite [32], but it is considered as negligible in both Owlshead and Noble Hills granites (which is in agreement with the arid climate and desertic environment) compared to hydrothermal activity.

At Soultz, [104] identified paleo-weathering at the top of the granite, between around 1400 and 1550 m depth, hence on a 150m thickness. There, the standard porphyritic granite is red colored as a result of paleo-weathering, because most of the primary iron-bearing minerals (biotite, magnetite, amphibole) are partly altered into iron-hydroxide or hematite. Seven kilometers away from Soultz, at Rittershoffen, in the same URG context, the top of the granitic basement between 2212 and 2269m (measured depth, MD) consists of a 56 m thick reddish granite [105] that was affected by a paleo-weathering alteration event because of paleo-emersion before and during the Permian [105]. It is characterized by a decreased magnetic content, as already measured on a continuous core at Soultz [11]. Gamma ray values encountered during well loging are high and close to 300 API units on average, a value also encountered for hydrothermal clay-rich sections with great abundance of illite. This paleo-weathering effect is also measurable through both the decreasing rate of penetration value

 doi:10.20944/preprints202308.2185.v1

during drilling associated with the declining influence of paleo-weathering and some of the well log responses such as the magnetic susceptibility log [104].

4. Carbonates

In addition to the nature and abundance of clay minerals [28,106] proved that the carbonate content is a good proxy for the hydrothermal alteration of granite bodies, in particular in the Rhine graben. It helps locate zones that have to be stimulated by acid treatment when it is necessary to improve the permeability of the reservoir through a better connectivity between wells and fractures. Indeed, in an Enhanced (or Engineered) Geothermal System (EGS), acid treatments dissolve carbonates that were naturally deposited in the fracture system and within its wall-rocks. This helps increasing the permeability and enhancing the capacity of geothermal brines to circulate within the granitic reservoir and to be produced at the surface. Indeed, [9,28,106] were the first authors to systematically analyze the carbonate content of a granite in the deep geothermal boreholes at Soultz by manocalcimetry. The average calcite content of a fresh granite is 0.252 wt.% and does not exceed 1.8 wt.% [107]. As a consequence, measurements above this latter value can be regarded as a calcite anomaly [106], due to hydrothermal alteration. Contents as high as 18 wt% in GPK-4 at Soultz are reported by [5,106] always in relation with fracture zones and correlated with fluid flow data obtained in the wells. These authors conclude that maximum calcite contents are similar and over 10 wt% in the three deep boreholes GPK-2, GPK-3 and GPK-4. However, GPK-3 and GPK-4 have a similar behavior as regards relationships between fracture zones, fluid flow and calcite content (the lower the calcite content, the better the fluid flow) that is opposite to that of GPK-2. This suggests that the fracture zones of GPK-3 and GPK-4 are localized and discrete while those of GPK-2 are a well-structured network of medium-scale fractures. The connectivity of these 3 wells to the fracture network may be different too. This difference of behavior between the 3 deep wells had also been illustrated by [108] who studied induced microseismicity. Hence, it might be very challenging to generalize what is learnt from a given well to the whole geothermal reservoir and to other reservoirs even in the same geological context. Subsequently calcite content was also included in reservoir assessment of Rittershoffen and Illkirch geothermal sites, also located in the URG [42,109]. In the NH granite, [6] indicate that the argillic alteration is highlighted by calcite content that increases together with porosity and temperature near fractures. They noted also the increase of the loss on ignition during bulk rock chemical analyses that indicates the degree of hydration of the rock correlated to a Na depletion due to plagioclase alteration and a K enrichment associated to illite crystallization.

Furthermore, carbonates trapped in small cavities the fluid from which they crystallized, allowing to characterize its salinity and trapping temperature thanks to microthermometry of those fluid inclusions. This technique was implemented by [24] to study the argillic alteration related to a cataclase zone of a sample collected at depth of 1641,91 m in EPS-1 drill hole at Soultz. At least three alteration stages are superimposed. The sample includes, from the oldest to the youngest as indicated by crosscutting relationships) a 3 mm-wide quartz vein, a 1 mm-wide ankerite vein and a thin vuggy quartz vein. The ankerite crystals clearly show a zonation of at least three crystallisation events. Inclusions show two phases (liquid + vapour) and have temperature of ice melting between –9,7 and +1°C, values higher than 0 °C being attributed to a metastable behaviour. Two groups of salinities were evidenced: salinity of about 10 wt% eq. NaCl, and salinity of less than 1 wt% eq. NaCl. A salinity of 10 wt% eq. NaCl is the present-day salinity of the fluids sampled in the granite and its sedimentary cover [110]. Very low salinities might correspond to meteoric water penetrating deeply due to rapidly opened fractures caused by seismic activity [24]. These variations could correspond to the mixing, at constant temperature, of sedimentary brines and meteoric waters [22,111]. Homogenization temperatures lie in a very narrow range around 145°C (137.5°C to 158°C) suggesting that inclusions have not been altered since their formation. Corrected from the effect of pressure, they indicate a temperature of fluid between 144°C and 159°C [24], intermediate between the present-day temperature of the fluid collected at the base of Triassic (120°C) and that harnessed in the deep reservoir at 5000m depth (200°C) at Soultz [48].

 doi:10.20944/preprints202308.2185.v1

5. Quartz

Partial sealing of fractures by secondary drusy quartz is a frequent sign of hydrothermal alteration in granitic environments [25,42,109,112,113]. Quartz cystals are easily detectable in rock-chips also called cuttings recovered from drilling operations by visual inspection, and in the laboratory by optical microscopy, fluid inclusion study and, isotopic measurements [22–25,114]. When cuttings are not available or reliable, gamma ray (GR) logging, which measures natural radioactivity in boreholes, is a good indicator of hydrothermal alteration. The occurrence of geodic quartz is associated with sharp localized GR negative anomalies, whereas K-bearing clay minerals are associated with positive anomalies that can extend several meters [104]. For example, one of the major permeable fracture zones of GPK-1 drill hole, located between 3489 and 3496m MD [115] is associated to mud losses but also occurrences of CH_4, CO_2 and radon [116]. GR presents a negative anomaly that corresponds to a quartz vein associated with the fracture [115]. The fracture zone is surrounded by two major open fractures with a highly altered zone in-between visible on flow logs and borehole imagery performed thanks to acoustic logging. Euhedral drusy quartz fragments were also found in the rock chips recovered during drilling at Rittershoffen at the same depths as temperature anomalies [42,112,117] indicating fluid flow and hence permeable zones. The permeability of the FZs seems to be influenced by the crystal growth of secondary quartz in fracture voids [118]. Indeed, these authors demonstrated by numerical simulations that due to the significant impact of the tortuosity - especially at lower sealing stages and even at identical relative sealing - the drop of fracture permeability is particularly pronounced for the needle quartz shape compared to the compact feature.

Like carbonates, quartz is able to trap the fluid it crystallized from in the form of fluid inclusions. At Soultz several microthermometry studies were performed on quartz samples [22,24,25]. Most of the fluid inclusions in secondary quartz crystals contain two phases (liquid + vapour) at room temperature, like those in ankerite [24]. All of the salinity and temperature values are rather consistent even though they sampled quartz veins at different depths in EPS-1 borehole. They are also consistent with data from ankerite [24]. Hence the temperature registered by quartz and ankerite correspond to the present-day temperature of the fluid circulating at present at the same depths in the granite body. Like for illite (see section 3.2.4), it is likely that quartz and carbonates continue precipitating at present in veins in the Soultz granite [24]. In order to provide additional data about flow paths and duration of interactions between the fluid and the granite other analyses can be performed like the determination of the isotopic signature of quartz [114].

In Bouillante, [68] identified an early potassic alteration facies typical of a high-temperature geothermal system characterized by newly formed K-feldspar/adularia + quartz + pyrite in which quartz textural properties revealed fracturing associated with at least two stages of boiling. In Terre-de-Haut, the study of 2 quartz generations was performed by microthermometry [99]. In a geodic euhedral quartz crystal, the hydrothermal fluid was of low salinity (2 wt% NaCl), probably of meteoric and sea water origin, at rather high temperature (240-270°C) in the core of the crystal and at lower temperature (ca 50°C) in its outer growth zone hence registering the cooling of the hydrothermal system. Additionally, a second type of fluid inclusions observed in a banded quartz vein indicated at least a hydrothermal episode with a CO_2-(H_2O) fluid, with traces of H_2S. Hence, some similarities can be highlighted between Terre-de-Haut and the Bouillante active geothermal systems in term of the highest temperatures of circulation events and gas composition, despite a difference in fluid origin (mostly meteoric in Terre-de-Haut [99], and combined magmatic, marine and meteoric in Bouillante [66]).

6. Discussion and conclusions

Following the examples presented before, newly formed minerals related to hydrothermal alteration are indeed very useful for the characterization of geothermal reservoirs (either active or fossil) and their cap-rock as they witnessed the conditions and duration of the events. In general, their detailed study is combined with other parameters such as petrophysical (like porosity, permeability, thermal conductivity) or geophysical (e.g. gamma ray) properties [1,29,66,119]. According to [1] the

Preprints (www.preprints.org) | NOT PEER-REVIEWED | Posted: 31 August 2023 doi:10.20944/preprints202308.2185.v1

advanced hydrothermal alteration of volcanic rocks like those found in Guadeloupe (Basse Terre and Terre-de-Haut) tends to increases fluid flow properties in lavas (by their increased porosity and permeability) and decreases them in volcano-sedimentary deposits. Hence hydrothermal alteration reduces significantly the differences in the thermo-physical properties observed between fresh facies in volcanics (lava flows and dykes, debris flows) and pyroclastics (ash, pumice and scoria deposits). The progressive transformation of primary minerals by hydrothermal alteration homogenizes the porous network by a reduction of pore throat diameters. In addition, after total alteration, the magnetic behaviour is fully diamagnetic or paramagnetic, leaving no remanent magnetization [1]. At Soultz, [82] showed the influence of hydrothermal alteration on the magnetic susceptibility of the granite and in particular the amount of clay minerals on its mechanical behavior.

Figure 6 is a synthesis of the factors and phenomena occurring at depth in a geothermal field developed in volcanic islands like Guadeloupe (Basse Terre and Terre-de-Haut) in subduction context. The recharge of the system occurs through rain and sea water. Water circulates thanks to faults and fractures and the topography is certainly promoting vertical water movements as evidenced for example by [120]. In addition, volcanic rock layers (lava flows, debris flows, pyroclastics) are superimposed on one another, some of them with rather high porosity, allowing horizontal water movements [1,29] which in addition to hydrothermal convection promote hydrothermal alteration halos along fractures. The core of the geothermal field shows the highest temperature, and the whole system is overlain by a rather impermeable clay cap mostly made of smectite [66,68] that ensures its perennity for a rather long period. Verati et al. (2016) an Favier et al. (2021) [3,102] assess a maximal timescale of about 400-450 ky for Les Saintes hydrothermalism, in agreement with both the timescale (~ 100 ky) proposed for active geothermal provinces in subduction context such as both the Taupo volcanic zone (New Zealand) [121] and Bouillante geothermal field [70].

The most used analytical means for the characterization of geothermal reservoirs and their clay-cap in the lab are XRD for clay minerals like smectite, illite, chlorite and inr-layered minerals, calcit and quartz , optical microscopy, scanning electron microscopy, microthermometry of fluid inclusions, K/Ar or Ar/Ar dating on illite or muscovite, use of chlorite geothermometer. Where boreholes are available, the data obtained in the lab are coupled with well-log and flow data to point out the most permeable zones and those that have to be stimulated.

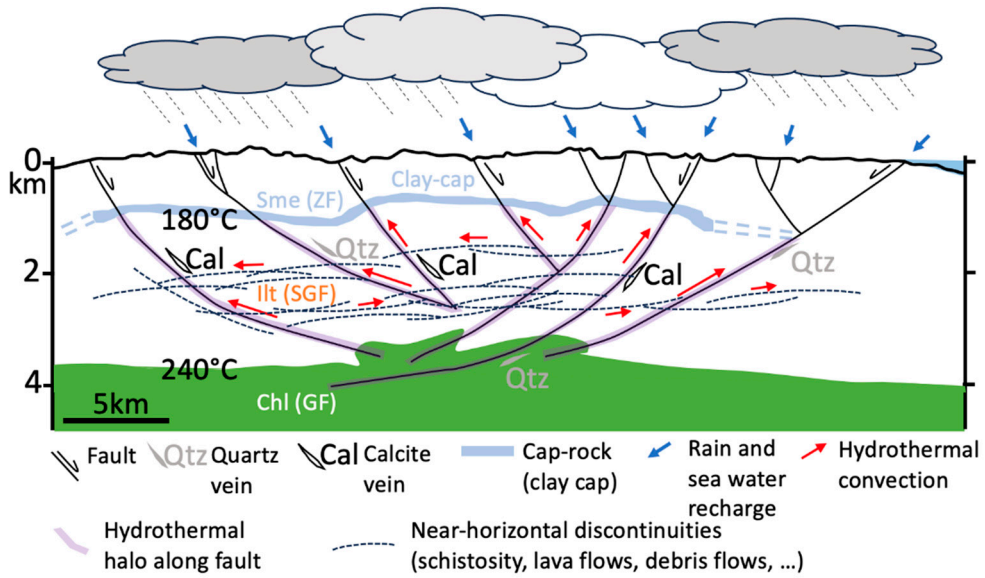

Figure 6. – Synthesis of factors and phenomena occurring at depth in a geothermal field developed in volcanic islands in subduction context, like Guadeloupe, after [13,29,66]. The depth may vary according to the authors as well as the temperature, hence they are only indicative. Sme: smectite, Ilt: illite, Chl : chlorite, Qtz: quartz, Cal : calcite, ZF : zeolite facies, SGF : sub-greenschist facies, GF : greenschist facies. Smectite, illite and chlorite are determined by XRD and chlorite (when associated

with quartz) is a good geothermometer. Quartz and calcite veins might provide fluid inclusions and hence temperature, salinity and composition of the fluid trapped during the crystallization of those minerals. Structural sketch after [29], clay-cap, 180°C and 240°C isotherms after [66], mineralogy after [13,29,66].

In addition to the various phenomena exposed before about clay minerals in crystalline rocks, another one can be encountered in geothermal reservoirs developed in deep sedimentary environments overlying granitic basements, like in the URG. In detrital geothermal reservoirs (sandstones, conglomerates), injectivity decline problems are often encountered during water reinjection into the subsurface, despite massive surface filtration. The reinjected water carries only nano-sized particles, like illite, at relatively low concentrations but causes severe permeability impairment due to pore clogging by the transported particles [122,123]. Nuclear Magnetic Resonance (NMR) is a powerful method to evaluate the clogging phenomena [124,125]. Independent NMR measurements allow to estimate the mean distance between the deposited clay particles and the reduction of this distance during clay injection reflecting the compaction of the deposit over time due to pore space particle accumulation [124]. Coupled NMR measurements and SEM imaging [124] allow to show where deposition occurs, for example on the surface of quartz grains or within pores and the shape and orientation of the deposits which contribute to permeability reduction and that threaten geothermal projects. This is very useful as [126] indicate in this issue that the oil reservoir quality is also reduced by the accumulation of mica flakes in the pore spaces.

Funding: This research was made in the framework of Geotref research and development project funded by the French Agency for Ecological Transition (ADEME, Investments for the Future). It is also included in the European Union's Horizon 2020 research and innovation program (Grant agreement No. 792037—MEET Project).

Data Availability Statement: "Not applicable.

Acknowledgments: Ms Nathalie Ouin is sincerely acknowledged for administrative support.

Conflicts of Interest: The author declares no conflict of interest. The funders had no role in the design of the study; in the collection, analyses, or interpretation of data; in the writing of the manuscript; or in the decision to publish the results.

References

1. Navelot, V.; Géraud, Y.; Favier, A.; Diraison, M.; Corsini, M.; Lardeaux, J.-M.; Verati, C.; Mercier de Lépinay, J.; Legendre, L.; Beauchamps, G. Petrophysical Properties of Volcanic Rocks and Impacts of Hydrothermal Alteration in the Guadeloupe Archipelago (West Indies). *Journal of Volcanology and Geothermal Research* **2018**, *360*, 1–21, doi:10.1016/j.jvolgeores.2018.07.004.
2. Favier, A.; Lardeaux, J.-M.; Corsini, M.; Verati, C.; Navelot, V.; Géraud, Y.; Diraison, M.; Ventalon, S.; Voitus, E. Characterization of an Exhumed High-Temperature Hydrothermal System and Its Application for Deep Geothermal Exploration: An Example from Terre-de-Haut Island (Guadeloupe Archipelago, Lesser Antilles Volcanic Arc). *Journal of Volcanology and Geothermal Research* **2021**, *418*, 107256, doi:10.1016/j.jvolgeores.2021.107256.
3. Verati, C.; Mazabraud, Y.; Lardeaux, J.-M.; Corsini, M.; Schneider, D.; Voitus, E.; Zami, F. Tectonic Evolution of Les Saintes Archipelago (Guadeloupe, French West Indies): Relation with the Lesser Antilles Arc System. *Bulletin de la Société Géologique de France* **2016**, *187*, 3–10, doi:10.2113/gssgfbull.187.1.3.
4. Genter, A.; Traineau, H.; Dezayes, C.; Elsass, P.; Ledesert, B.; Meunier, A.; Villemin, T. Fracture Analysis and Reservoir Characterization of the Granitic Basement in HDR Soultz Project (France). *Geothermal Science and Technology* **1995**, *4*, 189.
5. Hébert, R.L.; Ledésert, B.; Bartier, D.; Dezayes, C.; Genter, A.; Grall, C. The Enhanced Geothermal System of Soultz-Sous-Forêts: A Study of the Relationships between Fracture Zones and Calcite Content. *Journal of Volcanology and Geothermal Research* **2010**, *196*, 126–133, doi:10.1016/j.jvolgeores.2010.07.001.
6. Klee, J.; Chabani, A.; Ledésert, B.A.; Potel, S.; Hébert, R.L.; Trullenque, G. Fluid-Rock Interactions in a Paleo-Geothermal Reservoir (Noble Hills Granite, California, USA). Part 2: The Influence of Fracturing on Granite Alteration Processes and Fluid Circulation at Low to Moderate Regional Strain. *Geosciences* **2021**, *11*, 433, doi:10.3390/geosciences11110433.

7. Chabani, A.; Trullenque, G.; Ledésert, B.A.; Klee, J. Multiscale Characterization of Fracture Patterns: A Case Study of the Noble Hills Range (Death Valley, CA, USA), Application to Geothermal Reservoirs. *Geosciences* **2021**, *11*, 280.
8. Dezayes, C.; Villemin, T.; Pêcher, A. Microfracture Pattern Compared to Core-Scale Fractures in the Borehole of Soultz-Sous-Forêts Granite, Rhine Graben, France. *Journal of Structural Geology* **2000**, *22*, 723–733, doi:10.1016/S0191-8141(00)00003-1.
9. Ledésert, B.; Hebert, R.; Genter, A.; Bartier, D.; Clauer, N.; Grall, C. Fractures, Hydrothermal Alterations and Permeability in the Soultz Enhanced Geothermal System. *Comptes Rendus Geoscience* **2010**, *342*, 607–615.
10. Ledésert, B.; Dubois, J.; Genter, A.; Meunier, A. Fractal Analysis of Fractures Applied to Soultz-Sous-Forets Hot Dry Rock Geothermal Program. *Journal of Volcanology and Geothermal Research* **1993**, *57*, 1–17, doi:10.1016/0377-0273(93)90028-P.
11. Vidal, J.; Genter, A. Overview of Naturally Permeable Fractured Reservoirs in the Central and Southern Upper Rhine Graben: Insights from Geothermal Wells. *Geothermics* **2018**, *74*, 57–73, doi:10.1016/j.geothermics.2018.02.003.
12. Sardini, P.; Ledésert, B.; Touchard, G. Quantification of Microscopic Porous Networks By Image Analysis and Measurements of Permeability in the Soultz-Sous-Forêts Granite (Alsace, France). In *Fluid Flow and Transport in Rocks: Mechanisms and effects*; Jamtveit, B., Yardley, B.W.D., Eds.; Springer Netherlands: Dordrecht, 1997; pp. 171–189 ISBN 978-94-009-1533-6.
13. Beauchamps, G.; Ledésert, B.; Hébert, R.; Navelot, V.; Favier, A. The Characterisation of an Exhumed High-Temperature Paleo-Geothermal System on Terre-de-Haut Island (the Les Saintes Archipelago, Guadeloupe) in Terms of Clay Minerals and Petrophysics. *Geothermal Energy* **2019**, *7*, 1–18.
14. Beauchamps, G.; Bourdelle, F.; Dubois, M.; Hebert, R.L.; Ledésert, B.A. First Characterization of the Cooling of the Paleo-Geothermal System of Terre-de-Haut (Les Saintes Archipelago, Guadeloupe): Application of Fluid Inclusion and Chlorite Thermometry. *Journal of Volcanology and Geothermal Research* **2021**, *419*, 107370, doi:10.1016/j.jvolgeores.2021.107370.
15. Libbey, R.B.; Williams-Jones, A.E. Applications of Downhole Lithogeochemistry to Geothermal Exploration.
16. Maffucci, R.; Corrado, S.; Aldega, L.; Bigi, S.; Chiodi, A.; Di Paolo, L.; Giordano, G.; Invernizzi, C. Cap Rock Efficiency of Geothermal Systems in Fold-and-Thrust Belts: Evidence from Paleo-Thermal and Structural Analyses in Rosario de La Frontera Geothermal Area (NW Argentina). *Journal of Volcanology and Geothermal Research* **2016**, *328*, 84–95.
17. Corrado, S.; Aldega, L.; Celano, A.S.; De Benedetti, A.A.; Giordano, G. Cap Rock Efficiency and Fluid Circulation of Natural Hydrothermal Systems by Means of XRD on Clay Minerals (Sutri, Northern Latium, Italy). *Geothermics* **2014**, *50*, 180–188.
18. Weaver, J.; Eggertsson, G.H.; Utley, J.E.; Wallace, P.A.; Lamur, A.; Kendrick, J.E.; Tuffen, H.; Markússon, S.H.; Lavallée, Y. Thermal Liability of Hyaloclastite in the Krafla Geothermal Reservoir, Iceland: The Impact of Phyllosilicates on Permeability and Rock Strength. *Geofluids* **2020**, *2020*, 1–20.
19. Lévy, L.; Gibert, B.; Sigmundsson, F.; Flóvenz, Ó.; Hersir, G.; Briole, P.; Pezard, P. The Role of Smectites in the Electrical Conductivity of Active Hydrothermal Systems: Electrical Properties of Core Samples from Krafla Volcano, Iceland. *Geophysical Journal International* **2018**, *215*, 1558–1582, doi:10.1093/gji/ggy342.
20. Lévy, L.; Maurya, P.K.; Byrdina, S.; Vandemeulebrouck, J.; Sigmundsson, F.; Árnason, K.; Ricci, T.; Deldicque, D.; Roger, M.; Gibert, B. Electrical Resistivity Tomography and Time-Domain Induced Polarization Field Investigations of Geothermal Areas at Krafla, Iceland: Comparison to Borehole and Laboratory Frequency-Domain Electrical Observations. *Geophysical Journal International* **2019**, *218*, 1469–1489.
21. Carapezza, M.L.; Ranaldi, M.; Gattuso, A.; Pagliuca, N.M.; Tarchini, L. The Sealing Capacity of the Cap Rock above the Torre Alfina Geothermal Reservoir (Central Italy) Revealed by Soil CO2 Flux Investigations. *Journal of Volcanology and Geothermal Research* **2015**, *291*, 25–34.
22. Dubois, M.; Ayt Ougougdal, M.; Meere, P.; Royer, J.-J.; Boiron, M.-C.; Cathelineau, M. Temperature of Paleo- to Modern Self-Sealing within a Continental Rift Basin: The Fluid Inclusion Data (Soultz-Sous-Forêts, Rhine Graben, France). *ejm* **1996**, *8*, 1065–1080, doi:10.1127/ejm/8/5/1065.
23. Savary, V.; Dubois, M.; Ledésert, B.; Yardley, B.W.D.; Royer, J.-J. History of Fluid Circulation in an Alteration Zone of the Soultz-Sous-Forêts Granite (Alsace, France).; 1997; p. 292.
24. Dubois, M.; Ledésert, B.; Potdevin, J.-L.; Vançon, S. Détermination Des Conditions de Précipitation Des Carbonates Dans Une Zone d'altération Du Granite de Soultz (Soubassement Du Fossé Rhénan, France): L'enregistrement Des Inclusions Fluides. *Comptes Rendus de l'Académie des Sciences-Series IIA-Earth and Planetary Science* **2000**, *331*, 303–309.
25. Ledesert, B.; Berger, G.; Meunier, A.; Genter, A.; Bouchet, A. Diagenetic-Type Reactions Related to Hydrothermal Alteration in the Soultz-Sous-Forets Granite, France. *European Journal of Mineralogy* **1999**, *11*, 731–741.

26. Bottrell, S.H.; Yardley, B.W.D.; Buckley, F. A modified crush-leach method for the analysis of fluid inclusion electrolytes. *bulmi* **1988**, *111*, 279–290, doi:10.3406/bulmi.1988.8048.
27. Banks, D.A.; Yardley, B.W.D. Crush-Leach Analysis of Fluid Inclusions in Small Natural and Synthetic Samples. *Geochimica et Cosmochimica Acta* **1992**, *56*, 245–248, doi:10.1016/0016-7037(92)90129-7.
28. Hébert, R.; Ledésert, B.; Genter, A.; Bartier, D.; Dezayes, C. Mineral Precipitation in Geothermal Reservoir: The Study Case of Calcite in the Soultz-Sous-Forêts Enhanced Geothermal System.
29. Favier, A.; Lardeaux, J.-M.; Corsini, M.; Verati, C.; Navelot, V.; Géraud, Y.; Diraison, M.; Ventalon, S.; Voitus, E. Characterization of an Exhumed High-Temperature Hydrothermal System and Its Application for Deep Geothermal Exploration: An Example from Terre-de-Haut Island (Guadeloupe Archipelago, Lesser Antilles Volcanic Arc). *Journal of Volcanology and Geothermal Research* **2021**, *418*, 107256, doi:10.1016/j.jvolgeores.2021.107256.
30. A New Chlorite Geothermometer for Diagenetic to Low-Grade Metamorphic Conditions | SpringerLink Available online: https://link.springer.com/article/10.1007/s00410-012-0832-7 (accessed on 24 August 2023).
31. Inoue, A.; Kurokawa, K.; Hatta, T. Application of Chlorite Geothermometry to Hydrothermal Alteration in Toyoha Geothermal System, Southwestern Hokkaido, Japan. *Resource Geology* **2010**, *60*, 52–70, doi:10.1111/j.1751-3928.2010.00114.x.
32. Klee, J.; Potel, S.; Ledésert, B.A.; Hébert, R.L.; Chabani, A.; Barrier, P.; Trullenque, G. Fluid-Rock Interactions in a Paleo-Geothermal Reservoir (Noble Hills Granite, California, USA). Part 1: Granite Pervasive Alteration Processes Away from Fracture Zones. *Geosciences* **2021**, *11*, 325, doi:10.3390/geosciences11080325.
33. Peacock, D.C.P.; Sanderson, D.J.; Leiss, B. Use of Analogue Exposures of Fractured Rock for Enhanced Geothermal Systems. *Geosciences* **2022**, *12*, 318, doi:10.3390/geosciences12090318.
34. Ziegler, P.A. European Cenozoic Rift System. *Tectonophysics* **1992**, *208*, 91–111, doi:10.1016/0040-1951(92)90338-7.
35. Dèzes, P.; Schmid, S.M.; Ziegler, P.A. Evolution of the European Cenozoic Rift System: Interaction of the Alpine and Pyrenean Orogens with Their Foreland Lithosphere. *Tectonophysics* **2004**, *389*, 1–33, doi:10.1016/j.tecto.2004.06.011.
36. Baillieux, P.; Schill, E.; Edel, J.-B.; Mauri, G. Localization of Temperature Anomalies in the Upper Rhine Graben: Insights from Geophysics and Neotectonic Activity. *International Geology Review* **2013**, *55*, 1744–1762, doi:10.1080/00206814.2013.794914.
37. Benderitter, Y.; Elsass, P. Structural Control of Deep Fluid Circulation at the Soultz HDR Site, France: A Review. *International Journal of Rock Mechanics and Mining Sciences and Geomechanics Abstracts* **1996**, *3*, 104A.
38. Pribnow, D.; Clauser, C. HEAT AND FLUID FLOW AT THE SOULTZ HOT DRY ROCK SYSTEM IN THE RHINE GRABEN.
39. Pribnow, D.; Schellschmidt, R. Thermal Tracking of Upper Crustal Fluid Flow in the Rhine Graben. *Geophys. Res. Lett.* **2000**, *27*, 1957–1960, doi:10.1029/2000GL008494.
40. Baria, R.; Michelet, S.; Baumgaertner, J.; Dyer, B.; Nicholls, J.; Teza, D.; Hettkamp, T.; Soma, N.; Asanuma, H.; Kueperkoch, L. A 5000 m Deep Reservoir Development at the European HDR Site.
41. Baumgaertner, J.; Hettkamp, T.; Teza, D.; Koelbel, T.; Mergner, H.; Schlagermann, P.; Lerch, C.; Pfalzwerke geofuture GmbH, L. Operational experiences with the geothermal power plants Landau, Insheim and Bruchsal; Betriebserfahrungen mit den Geothermiekraftwerken Landau, Insheim und Bruchsal. *bbr. Leitungsbau, Brunnenbau, Geothermie* **2013**, *64*.
42. Vidal, J.; Genter, A.; Chopin, F. Permeable Fracture Zones in the Hard Rocks of the Geothermal Reservoir at Rittershoffen, France: Permeable Fracture Zones, Rittershoffen. *J. Geophys. Res. Solid Earth* **2017**, *122*, 4864–4887, doi:10.1002/2017JB014331.
43. Gerard, A.; Kappelmeyer, O. The Soultz-Sous-Forets Project. *Geothermics* **1987**, *16*, 393–399, doi:10.1016/0375-6505(87)90018-6.
44. Evans, K.F.; Genter, A.; Sausse, J. Permeability Creation and Damage Due to Massive Fluid Injections into Granite at 3.5 Km at Soultz: 1. Borehole Observations: PERMEABILITY CREATION IN GRANITE. *J. Geophys. Res.* **2005**, *110*, doi:10.1029/2004JB003168.
45. Kushnir, A.R.L.; Heap, M.J.; Baud, P. Assessing the Role of Fractures on the Permeability of the Permo-Triassic Sandstones at the Soultz-Sous-Forêts (France) Geothermal Site. *Geothermics* **2018**, *74*, 181–189, doi:10.1016/j.geothermics.2018.03.009.
46. *Geothermal Energy Systems: Exploration, Development, and Utilization*; Huenges, E., Ed.; 1st ed.; Wiley, 2010; ISBN 978-3-527-40831-3.
47. Baillieux, P.; Schill, E.; Abdelfettah, Y.; Dezayes, C. Possible Natural Fluid Pathways from Gravity Pseudo-Tomography in the Geothermal Fields of Northern Alsace (Upper Rhine Graben). *Geotherm Energy* **2014**, *2*, 16, doi:10.1186/s40517-014-0016-y.
48. Ledésert, B.A.; Hébert, R.L. How Can Deep Geothermal Projects Provide Information on the Temperature Distribution in the Upper Rhine Graben? The Example of the Soultz-Sous-Forêts-Enhanced Geothermal System. *Geosciences* **2020**, *10*, 459, doi:10.3390/geosciences10110459.

49. Norton, I. Two-Stage Formation of Death Valley. *Geosphere* **2011**, *7*, 171–182, doi:10.1130/GES00588.1.
50. Dokka, R.K.; Travis, C.J. Role of the Eastern California Shear Zone in Accommodating Pacific-North American Plate Motion. *Geophys. Res. Lett.* **1990**, *17*, 1323–1326, doi:10.1029/GL017i009p01323.
51. Stewart, J.H.; Ernst, W.G. Tectonics of the Walker Lane Belt, Western Great Basin: Mesozoic and Cenozoic Deformation in a Zone of Shear. *Metamorphism and crustal evolution of the western United States* **1988**, *7*, 683–713.
52. Lifton, Z.M.; Newman, A.V.; Frankel, K.L.; Johnson, C.W.; Dixon, T.H. Insights into Distributed Plate Rates across the Walker Lane from GPS Geodesy: WALKER LANE GPS. *Geophys. Res. Lett.* **2013**, *40*, 4620–4624, doi:10.1002/grl.50804.
53. Miller, M.M.; Johnson, D.J.; Dixon, T.H.; Dokka, R.K. Refined Kinematics of the Eastern California Shear Zone from GPS Observations, 1993-1998. *J. Geophys. Res.* **2001**, *106*, 2245–2263, doi:10.1029/2000JB900328.
54. Hill, M.L.; Troxel, B.W. TECTONICS OF DEATH VALLEY REGION, CALIFORNIA. *Geol Soc America Bull* **1966**, *77*, 435, doi:10.1130/0016-7606(1966)77[435:TODVRC]2.0.CO;2.
55. Burchfiel, B.C.; Stewart, J.H. "PULL-APART" ORIGIN OF THE CENTRAL SEGMENT OF DEATH VALLEY, CALIFORNIA. *Geol Soc America Bull* **1966**, *77*, 439, doi:10.1130/0016-7606(1966)77[439:POOTCS]2.0.CO;2.
56. Pavlis, T.L.; Trullenque, G. Evidence for 40–41 Km of Dextral Slip on the Southern Death Valley Fault: Implications for the Eastern California Shear Zone and Extensional Tectonics. *Geology* **2021**, *49*, 767–772, doi:10.1130/G48528.1.
57. Rämö, T.O.; Calzia, J.P.; Kosunen, P.J. Geochemistry of Mesozoic Plutons, Southern Death Valley Region, California: Insights into the Origin of Cordilleran Interior Magmatism. *Contrib Mineral Petrol* **2002**, *143*, 416–437, doi:10.1007/s00410-002-0354-9.
58. Troxel, B.W.; Butler, P.R. *Rate of Cenozoic Slip on Normal Faults, South-Central Death Valley, California*; Department of Geology, University of California, 1979;
59. Chabani, A.; Trullenque, G.; Klee, J.; Ledésert, B.A. Fracture Spacing Variability and the Distribution of Fracture Patterns in Granitic Geothermal Reservoir: A Case Study in the Noble Hills Range (Death Valley, CA, USA). *Geosciences* **2021**, *11*, 520, doi:10.3390/geosciences11120520.
60. Bouysse, P.; Guennoc, P. Donnees sur la structure de l'arc insulaire des Petites Antilles, entre Ste-Lucie et Anguilla. *Marine Geology* **1983**, *53*, 131–166, doi:10.1016/0025-3227(83)90038-5.
61. Hawkesworth, C.J.; Powell, M. Magma Genesis in the Lesser Antilles Island Arc. *Earth and Planetary Science Letters* **1980**, *51*, 297–308, doi:10.1016/0012-821X(80)90212-5.
62. DeMets, C.; Jansma, P.E.; Mattioli, G.S.; Dixon, T.H.; Farina, F.; Bilham, R.; Calais, E.; Mann, P. GPS Geodetic Constraints on Caribbean-North America Plate Motion. *Geophys. Res. Lett.* **2000**, *27*, 437–440, doi:10.1029/1999GL005436.
63. Symithe, S.; Calais, E.; De Chabalier, J.B.; Robertson, R.; Higgins, M. Current Block Motions and Strain Accumulation on Active Faults in the Caribbean: CURRENT CARIBBEAN KINEMATICS. *J. Geophys. Res. Solid Earth* **2015**, *120*, 3748–3774, doi:10.1002/2014JB011779.
64. Sanjuan, B.; Traineau, H. Development of the Bouillante Geothermal Field (Guadeloupe, French West Indies). *IGA News* **2008**, 5–9.
65. Bremner, P.R.; Schultze, L.E.; Ming, D.W.; Mumpton, F.A. Ability of Clinoptilolite-Rich Tuffs to Remove Metal Cations Commonly Found in Acidic Drainage. *Natural zeolites* **1995**, *93*, 397–403.
66. Bouchot, V.; Traineau, H.; Guillou-Frottier, L.; Thinon, I.; Baltassat, J.-M.; Fabriol, H.; Bourgeois, B.; Lasne, E. Assessment of the Bouillante Geothermal Field (Guadeloupe, French West Indies): Toward a Conceptual Model of the High Temperature Geothermal System.
67. Thinon, I.; Guennoc, P.; Bitri, A.; Truffert, C. Study of the Bouillante Bay (West Basse-Terre Island Shelf): Contribution of Geophysical Surveys to the Understanding of the Structural Context of Guadeloupe (French West Indies - Lesser Antilles). *Bulletin de la Société Géologique de France* **2010**, *181*, 51–65, doi:10.2113/gssgfbull.181.1.51.
68. Patrier, P.; Bruzac, S.; Pays, R.; Beaufort, D.; Bouchot, V.; Verati, C.; Gadalia, A. Occurrence of K-Feldspar-Bearing Hydrothermal Breccias in the Bouillante Geothermal Field (Basse Terre – Guadeloupe). *Bulletin de la Société Géologique de France* **2013**, *184*, 119–128, doi:10.2113/gssgfbull.184.1-2.119.
69. Samper, A.; Quidelleur, X.; Lahitte, P.; Mollex, D. Timing of Effusive Volcanism and Collapse Events within an Oceanic Arc Island: Basse-Terre, Guadeloupe Archipelago (Lesser Antilles Arc). *Earth and Planetary Science Letters* **2007**, *258*, 175–191, doi:10.1016/j.epsl.2007.03.030.
70. Verati, C.; Patrier-Mas, P.; Lardeaux, J.M.; Bouchot, V. Timing of Geothermal Activity in an Active Island-Arc Volcanic Setting: First 40Ar/39Ar Dating from Bouillante Geothermal Field (Guadeloupe, French West Indies). *Geological Society, London, Special Publications* **2014**, *378*, 285–295, doi:10.1144/SP378.19.
71. Zami, F.; Quidelleur, X.; Ricci, J.; Lebrun, J.-F.; Samper, A. Initial Sub-Aerial Volcanic Activity along the Central Lesser Antilles Inner Arc: New K–Ar Ages from Les Saintes Volcanoes. *Journal of Volcanology and Geothermal Research* **2014**, *287*, 12–21, doi:10.1016/j.jvolgeores.2014.09.011.

72. Strangway, D.W.; Swift, C.M.; Holmer, R.C. THE APPLICATION OF AUDIO-FREQUENCY MAGNETOTELLURICS (AMT) TO MINERAL EXPLORATION. *GEOPHYSICS* **1973**, *38*, 1159–1175, doi:10.1190/1.1440402.
73. Lee, T.J.; Song, Y.; Uchida, T. Three-Dimensional Magnetotelluric Surveys for Geothermal Development in Pohang, Korea. *Exploration Geophysics* **2007**, *38*, 89–97, doi:10.1071/EG07004.
74. Lee, T.J.; Han, N.; Song, Y. Magnetotelluric Survey Applied to Geothermal Exploration: An Example at Seokmo Island, Korea. *Exploration Geophysics* **2010**, *41*, 61–68, doi:10.1071/EG10001.
75. Amatyakul, P.; Rung-Arunwan, T.; Siripunvaraporn, W. A Pilot Magnetotelluric Survey for Geothermal Exploration in Mae Chan Region, Northern Thailand. *Geothermics* **2015**, *55*, 31–38, doi:10.1016/j.geothermics.2015.01.009.
76. Patro, P.K. Magnetotelluric Studies for Hydrocarbon and Geothermal Resources: Examples from the Asian Region. *Surv Geophys* **2017**, *38*, 1005–1041, doi:10.1007/s10712-017-9439-x.
77. Gailler, L.-S.; Bouchot, V.; Martelet, G.; Thinon, I.; Coppo, N.; Baltassat, J.-M.; Bourgeois, B. Contribution of Multi-Method Geophysics to the Understanding of a High-Temperature Geothermal Province: The Bouillante Area (Guadeloupe, Lesser Antilles). *Journal of Volcanology and Geothermal Research* **2014**, *275*, 34–50, doi:10.1016/j.jvolgeores.2014.02.002.
78. Patrier, P.; Beaufort, D.; Mas, A.; Traineau, H. Surficial Clay Assemblage Associated with the Hydrothermal Activity of Bouillante (Guadeloupe, French West Indies). *Journal of Volcanology and Geothermal Research* **2003**, *126*, 143–156, doi:10.1016/S0377-0273(03)00133-1.
79. Mas, A.; Guisseau, D.; Patrier Mas, P.; Beaufort, D.; Genter, A.; Sanjuan, B.; Girard, J.P. Clay Minerals Related to the Hydrothermal Activity of the Bouillante Geothermal Field (Guadeloupe). *Journal of Volcanology and Geothermal Research* **2006**, *158*, 380–400, doi:10.1016/j.jvolgeores.2006.07.010.
80. Glaas, C.; Vidal, J.; Genter, A. Structural Characterization of Naturally Fractured Geothermal Reservoirs in the Central Upper Rhine Graben. *Journal of Structural Geology* **2021**, *148*, 104370, doi:10.1016/j.jsg.2021.104370.
81. Ledésert, B.; Joffre, J.; Amblès, A.; Sardini, P.; Genter, A.; Meunier, A. Organic Matter in the Soultz HDR Granitic Thermal Exchanger (France): Natural Tracer of Fluid Circulations between the Basement and Its Sedimentary Cover. *Journal of Volcanology and Geothermal Research* **1996**, *70*, 235–253, doi:10.1016/0377-0273(95)00058-5.
82. Meller, C.; Kohl, T. The Significance of Hydrothermal Alteration Zones for the Mechanical Behavior of a Geothermal Reservoir. *Geotherm Energy* **2014**, *2*, 12, doi:10.1186/s40517-014-0012-2.
83. Berger, G.; Velde, B. Chemical Parameters Controlling the Propylitic and Argillic Alteration Process. *European Journal of Mineralogy* **1992**, 1439–1456, doi:10.1127/ejm/4/6/1439.
84. Sanjuan, B.; Millot, R.; Dezayes, C.; Brach, M. Main Characteristics of the Deep Geothermal Brine (5km) at Soultz-Sous-Forêts (France) Determined Using Geochemical and Tracer Test Data. *Comptes Rendus Geoscience* **2010**, *342*, 546–559, doi:10.1016/j.crte.2009.10.009.
85. Mouchot, J.; Genter, A.; Cuenot, N.; Scheiber, J.; Seibel, O.; Bosia, C.; Ravier, G. First Year of Operation from EGS Geothermal Plants in Alsace, France: Scaling Issues.
86. Sanjuan, B.; Millot, R.; Innocent, Ch.; Dezayes, Ch.; Scheiber, J.; Brach, M. Major Geochemical Characteristics of Geothermal Brines from the Upper Rhine Graben Granitic Basement with Constraints on Temperature and Circulation. *Chemical Geology* **2016**, *428*, 27–47, doi:10.1016/j.chemgeo.2016.02.021.
87. Tracer Testing of the EGS Site at Soultz-Sous-Forêts (Alsace, France) between 2005 and 2013 - BRGM - Bureau de Recherches Géologiques et Minières Available online: https://brgm.hal.science/hal-01074104/ (accessed on 26 August 2023).
88. Fritz, B.; Jacquot, E.; Jacquemont, B.; Baldeyrou-Bailly, A.; Rosener, M.; Vidal, O. Geochemical Modelling of Fluid–Rock Interactions in the Context of the Soultz-Sous-Forêts Geothermal System. *Comptes Rendus Geoscience* **2010**, *342*, 653–667, doi:10.1016/j.crte.2010.02.005.
89. Genter, A.; Traineau, H. Analysis of Macroscopic Fractures in Granite in the HDR Geothermal Well EPS-1, Soultz-Sous-Foreˆts, France. *Journal of Volcanology and Geothermal Research* **1996**, *72*, 121–141, doi:10.1016/0377-0273(95)00070-4.
90. Bartier, D.; Ledésert, B.; Clauer, N.; Meunier, A.; Liewig, N.; Morvan, G.; Addad, A. Hydrothermal Alteration of the Soultz-Sous-Forêts Granite (Hot Fractured Rock Geothermal Exchanger) into a Tosudite and Illite Assemblage. *European Journal of Mineralogy* **2008**, *20*, 131–142, doi:10.1127/0935-1221/2008/0020-1787.
91. Merceron, T.; Inoue, A.; Bouchet, A.; Meunier, A. Lithium-Bearing Donbassite and Tosudite from Echassières, Massif Central, France. *Clays Clay Miner.* **1988**, *36*, 39–46, doi:10.1346/CCMN.1988.0360106.
92. Creach, M.; Meunier, A.; Beaufort, D. Tosudite Crystallization in the Kaolinized Granitic Cupola of Montebras, Creuse, France. *Clay Minerals* **1986**, *21*, 225–230, doi:10.1180/claymin.1986.021.2.11.
93. Ichikawa, A.; Shimoda, S. Tosudite from the Hokuno Mine, Hokuno, Gifu Prefecture, Japan. *Clays Clay Miner.* **1976**, *24*, 142–148, doi:10.1346/CCMN.1976.0240307.
94. Shimoda, S. New Data for Tosudite. *Clays Clay Miner.* **1969**, *17*, 179–184, doi:10.1346/CCMN.1969.0170306.

95. Cruz, M.D.R.; Andreo, B. Tosudite in Very Low-Grade Metamorphic Graywackes from the Malaga Area (Betic Cordilleras, Spain). *European Journal of Mineralogy* **1997**, 1391–1400, doi:10.1127/ejm/8/6/1391.
96. Fries, D.; Lebouil, S.; Maurer, V.; Martin, C.; Baujard, C.; Ravier, G.; Boguais, R.; Amari, S. *Lithium Extraction through Pilot Scale Tests under Real Geothermal Conditions of the Upper Rhine Graben*; 2022;
97. Toba, A.-L.; Nguyen, R.T.; Cole, C.; Neupane, G.; Paranthaman, M.P. U.S. Lithium Resources from Geothermal and Extraction Feasibility. *Resources, Conservation and Recycling* **2021**, *169*, 105514, doi:10.1016/j.resconrec.2021.105514.
98. Lanari, P.; Wagner, T.; Vidal, O. A Thermodynamic Model for Di-Trioctahedral Chlorite from Experimental and Natural Data in the System MgO–FeO–Al2O3–SiO2–H2O: Applications to P–T Sections and Geothermometry. *Contrib Mineral Petrol* **2014**, *167*, 968, doi:10.1007/s00410-014-0968-8.
99. Beauchamps, G.; Bourdelle, F.; Dubois, M.; Hebert, R.L.; Ledésert, B.A. First Characterization of the Cooling of the Paleo-Geothermal System of Terre-de-Haut (Les Saintes Archipelago, Guadeloupe): Application of Fluid Inclusion and Chlorite Thermometry. *Journal of Volcanology and Geothermal Research* **2021**, *419*, 107370, doi:10.1016/j.jvolgeores.2021.107370.
100. Drits, V. XRD Measurement of Mean Crystallite Thickness of Illite and Illite/Smectite: Reappraisal of the Kubler Index and the Scherrer Equation. *Clays and Clay Minerals* **1997**, *45*, 461–475, doi:10.1346/CCMN.1997.0450315.
101. Clauer, N.; Liewig, N.; Ledesert, B.; Zwingmann, H. Thermal History of Triassic Sandstones from the Vosges Mountains-Rhine Graben Rifting Area, NE France, Based on K-Ar Illite Dating. *Clay miner.* **2008**, *43*, 363–379, doi:10.1180/claymin.2008.043.3.03.
102. Favier, A.; Verati, C.; Lardeaux, J.-M.; Münch, P.; Renac, C.; Corsini, M.; Orange, F. 40Ar/39Ar Dating of High Temperature Geothermal Systems: First Attempt on Hydrothermally Altered Pyroxenes from the Saintes Archipelago (Lesser Antilles Arc, Guadeloupe). *Chemical Geology* **2021**, *581*, 120401, doi:10.1016/j.chemgeo.2021.120401.
103. Guisseau, D.; Patrier Mas, P.; Beaufort, D.; Girard, J.P.; Inoue, A.; Sanjuan, B.; Petit, S.; Lens, A.; Genter, A. Significance of the Depth-Related Transition Montmorillonite-Beidellite in the Bouillante Geothermal Field (Guadeloupe, Lesser Antilles). *American Mineralogist* **2007**, *92*, 1800–1813.
104. Hooijkaas, G.R.; Genter, A.; Dezayes, C. Deep-Seated Geology of the Granite Intrusions at the Soultz EGS Site Based on Data from 5km-Deep Boreholes. *Geothermics* **2006**, *35*, 484–506, doi:10.1016/j.geothermics.2006.03.003.
105. Duringer, P.; Aichholzer, C.; Orciani, S.; Genter, A. The Complete Lithostratigraphic Section of the Geothermal Wells in Rittershoffen (Upper Rhine Graben, Eastern France): A Key for Future Geothermal Wells. *BSGF - Earth Sci. Bull.* **2019**, *190*, 13, doi:10.1051/bsgf/2019012.
106. Ledésert, B.; Hébert, R.L.; Grall, C.; Genter, A.; Dezayes, C.; Bartier, D.; Gérard, A. Calcimetry as a Useful Tool for a Better Knowledge of Flow Pathways in the Soultz-Sous-Forêts Enhanced Geothermal System. *Journal of Volcanology and Geothermal Research* **2009**, *181*, 106–114, doi:10.1016/j.jvolgeores.2009.01.001.
107. White, A.F.; Schulz, M.S.; Lowenstern, J.B.; Vivit, D.V.; Bullen, T.D. The Ubiquitous Nature of Accessory Calcite in Granitoid Rocks: Implications for Weathering, Solute Evolution, and Petrogenesis. *Geochimica et Cosmochimica Acta* **2005**, *69*, 1455–1471, doi:10.1016/j.gca.2004.09.012.
108. Dorbath, L.; Cuenot, N.; Genter, A.; Frogneux, M. Seismic Response of the Fractured and Faulted Granite to Massive Water Injection at 5 Km Depth at Soultz-Sous-Forêts (France). *Geophysical Journal International* **2009**, *177*, 653–675.
109. Glaas, C.; Patrier, P.; Vidal, J.; Beaufort, D.; Girard, J.-F.; Genter, A. Hydrothermal Alteration in the New Deep Geothermal Well GIL-1 (Strasbourg Area, France). In Proceedings of the Proceedings World Geothermal Congress; 2020.
110. Pauwels, H.; Fouillac, C.; Fouillac, A.-M. Chemistry and Isotopes of Deep Geothermal Saline Fluids in the Upper Rhine Graben: Origin of Compounds and Water-Rock Interactions. *Geochimica et Cosmochimica Acta* **1993**, *57*, 2737–2749, doi:10.1016/0016-7037(93)90387-C.
111. Cathelineau, M.; Boiron, M.-C. Downward Penetration and Mixing of Sedimentary Brines and Dilute Hot Waters at 5km Depth in the Granite Basement at Soultz-Sous-Forêts (Rhine Graben, France). *Comptes Rendus Geoscience* **2010**, *342*, 560–565, doi:10.1016/j.crte.2009.08.010.
112. Vidal, J.; Genter, A.; Schmittbuhl, J. Pre- and Post-Stimulation Characterization of Geothermal Well GRT-1, Rittershoffen, France: Insights from Acoustic Image Logs of Hard Fractured Rock. *Geophysical Journal International* **2016**, *206*, 845–860, doi:10.1093/gji/ggw181.
113. Klee, J.; Chabani, A.; Ledésert, B.A.; Potel, S.; Hébert, R.L.; Trullenque, G. Fluid-Rock Interactions in a Paleo-Geothermal Reservoir (Noble Hills Granite, California, USA). Part 2: The Influence of Fracturing on Granite Alteration Processes and Fluid Circulation at Low to Moderate Regional Strain. *Geosciences* **2021**, *11*, 433, doi:10.3390/geosciences11110433.
114. Smith, M.P.; Savary, V.; Yardley, B.W.D.; Valley, J.W.; Royer, J.J.; Dubois, M. The Evolution of the Deep Flow Regime at Soultz-Sous-Forêts, Rhine Graben, Eastern France: Evidence from a Composite Quartz Vein. *J. Geophys. Res.* **1998**, *103*, 27223–27237, doi:10.1029/98JB02528.

115. Dezayes, C.; Genter, A.; Valley, B. Structure of the Low Permeable Naturally Fractured Geothermal Reservoir at Soultz. *Comptes Rendus Geoscience* **2010**, *342*, 517–530, doi:10.1016/j.crte.2009.10.002.
116. Vidal, J.; Genter, A. Overview of Naturally Permeable Fractured Reservoirs in the Central and Southern Upper Rhine Graben: Insights from Geothermal Wells. *Geothermics* **2018**, *74*, 57–73, doi:10.1016/j.geothermics.2018.02.003.
117. Glaas, C.; Vidal, J.; Patrier, P.; Girard, J.-F.; Beaufort, D.; Petit, S.; Genter, A. How Do Secondary Minerals in Granite Help Distinguish Paleo- from Present-Day Permeable Fracture Zones? Joint Interpretation of SWIR Spectroscopy and Geophysical Logs in the Geothermal Wells of Northern Alsace. *Geofluids* **2019**, *2019*, 1–20, doi:10.1155/2019/8231816.
118. Kling, T.; Schwarz, J.-O.; Wendler, F.; Enzmann, F.; Blum, P. Fracture Flow Due to Hydrothermally Induced Quartz Growth. *Advances in Water Resources* **2017**, *107*, 93–107, doi:10.1016/j.advwatres.2017.06.011.
119. Meller, C.; Ledésert, B. Is There a Link between Mineralogy, Petrophysics, and the Hydraulic and Seismic Behaviors of the Soultz-Sous-Forêts Granite during Stimulation? A Review and Reinterpretation of Petro-Hydromechanical Data toward a Better Understanding of Induced Seismicity and Fluid Flow. *Journal of Geophysical Research: Solid Earth* **2017**, *122*, 9755–9774.
120. Taillefer, A.; Guillou-Frottier, L.; Soliva, R.; Magri, F.; Lopez, S.; Courrioux, G.; Millot, R.; Ladouche, B.; Le Goff, E. Topographic and Faults Control of Hydrothermal Circulation Along Dormant Faults in an Orogen. *Geochem. Geophys. Geosyst.* **2018**, doi:10.1029/2018GC007965.
121. Rowland, J.V.; Sibson, R.H. Structural Controls on Hydrothermal Flow in a Segmented Rift System, Taupo Volcanic Zone, New Zealand. *Geofluids* **2004**, *4*, 259–283, doi:10.1111/j.1468-8123.2004.00091.x.
122. Ines, R.; Eric, K.; Marc, F.; Nicolas, P.; Béatrice, L. Formation Damage Induced by Clay Colloids Deposition in Triassic Clastic Geothermal Fields: Insights from an Experimental Approach. *Applied Clay Science* **2023**, *234*, 106868, doi:10.1016/j.clay.2023.106868.
123. Du, X.; Ye, X.; Zhang, X. Clogging of Saturated Porous Media by Silt-Sized Suspended Solids under Varying Physical Conditions during Managed Aquifer Recharge. *Hydrological Processes* **2018**, *32*, 2254–2262, doi:10.1002/hyp.13162.
124. Ines, R.; Marc, F.; Eric, K.; Nicolas, P.; Béatrice, L. Clay-Induced Permeability Decline in Sandstone Reservoirs: Insights from a Coupled NMR-SEM Experimental Approach. *Geothermics* **2023**, *114*, 102784, doi:10.1016/j.geothermics.2023.102784.
125. Adebayo, A.R.; Bageri, B.S. A Simple NMR Methodology for Evaluating Filter Cake Properties and Drilling Fluid-Induced Formation Damage. *J Petrol Explor Prod Technol* **2020**, *10*, 1643–1655, doi:10.1007/s13202-019-00786-3.
126. Opuwari, M.; Ubong, M.O.; Jamjam, S.; Magoba, M. The Impact of Detrital Minerals on Reservoir Flow Zones in the Northeastern Bredasdorp Basin, South Africa, Using Core Data. *Minerals* **2022**, *12*, 1009, doi:10.3390/min12081009.